A Novel Cyclic Biased Agonist of the Apelin Receptor, MM07, is Disease Modifying in the Rat Monocrotaline Model of Pulmonary Arterial Hypertension

Running Title: MM07, a G protein biased apelin agonist is beneficial in PAH

Peiran Yang[1] PhD, Cai Read[1] MRes, Rhoda E Kuc[1] GI Biol, Duuamene Nyimanu[1] MSc, Thomas L Williams[1] MRes, Alexi Crosby[2] PhD, Guido Buonincontri[3] PhD, Mark Southwood[4] PhD, Stephen J Sawiak[3] PhD, Robert C. Glen[5] PhD, Nicholas W Morrell[2] MD, Anthony P Davenport[1] PhD, Janet J Maguire[1] PhD

P Yang* and C Read should be considered as joint first author. AP Davenport and JJ Maguire should be considered as joint senior author.

[1]Experimental Medicine and Immunotherapeutics, University of Cambridge, Level 6, Centre for Clinical Investigation, Box 110, Addenbrooke's Hospital, Cambridge, CB2 0QQ, U.K.

[2]Department of Medicine, University of Cambridge, Box 157, Addenbrooke's Hospital, Cambridge, CB2 0QQ, U.K.

[3]Wolfson Brain Imaging Centre, Department of Clinical Neuroscience, University of Cambridge, Box 65, CB2 0QQ, Cambridge, U.K.

[4]Department of Pathology, Papworth Hospital, Papworth Everard, Cambridge, CB23 8RE, U.K.

[5]The Centre for Molecular Informatics, Department of Chemistry, University of Cambridge, Cambridge, UK and Computational and Systems Medicine, Department of Surgery and Cancer, Faculty of Medicine, Imperial College London, UK.

*Current address: Division of Cardiovascular Medicine, Department of Medicine, Brigham and Women's Hospital and Harvard Medical School, Boston, MA, 02115, USA.

Corresponding author: Dr Janet J Maguire
Experimental Medicine and Immunotherapeutics,
University of Cambridge,
Level 6, Centre for Clinical Investigation,

Box 110, Addenbrooke's Hospital,
Cambridge, CB2 0QQ, UK.
Fax: +44 (0)1223 761576
Phone: +44 (0)1223 336899
Email: jjm1003@medschl.cam.ac.uk

Acknowledgments

This work was supported by the Medical Research Council MC_PC_14116 [to APD] Wellcome Trust [107715/Z/15/Z to APD], Programme in Metabolic and Cardiovascular Disease [096822/Z/11/Z to PY; 203814/Z/16/A to TLW], Parke Davis Fellowship [to PY], British Heart Foundation [FS/14/59/31282 to CR] and in part by the National Institute for Health Research Cambridge Biomedical Research Centre.

Author Contributions; PY, CR, REK, DN, TLW, AC, GB, MS, SJS, NWM, APD and JJM have made substantial contributions to conception and design or acquisition of data, or analysis and interpretation of data. R.C.G. design of MM07. PY, CR, APD and JJM were involved in drafting the manuscript or revising it critically for important intellectual content.

Conflict of Interest None

Declaration of transparency and scientific rigour

This Declaration acknowledges that this paper adheres to the principles for transparent reporting and scientific rigour of preclinical research recommended by funding agencies, publishers and other organisations engaged with supporting research.

Bullet point summary

'What is already known'

- Apelin is down regulated in pulmonary arterial hypertension.

'What this study adds'

- A G protein-biased apelin peptide agonist is disease modifying in a model of PAH

‘Clinical significance’

- Supports the development of G protein-biased apelin agonists for treatment of PAH.

Abstract 250 words

Background and Purpose: Apelin is an endogenous vasodilatory and inotropic peptide that is down-regulated in human pulmonary arterial hypertension, however, the density of the apelin receptor is not significantly attenuated. We hypothesised that a G protein-biased apelin analogue MM07, which is more stable than the endogenous apelin peptide, may be beneficial in this condition with the advantage of reduced β-arrestin mediated receptor internalisation with chronic use.

Experimental Approach: Male Sprague-Dawley rats received either monocrotaline to induce pulmonary arterial hypertension or saline and then daily intraperitoneal injections of either MM07 or saline for 21 days. The extent of disease was assessed by right ventricular catheterisation, cardiac MRI and histological analysis of the pulmonary vasculature. The effect of MM07 on signalling, proliferation and apoptosis of human pulmonary artery endothelial cells was investigated.

Key Results: MM07 significantly reduced the elevation of right ventricular systolic pressure and hypertrophy induced by monocrotaline. Monocrotaline-induced changes in cardiac structure and function, including right ventricular end-systolic and end-diastolic volumes, ejection fraction and left ventricular end-diastolic volume, were attenuated by MM07. MM07 also significantly reduced monocrotaline-induced muscularisation of small pulmonary blood vessels. MM07 stimulated endothelial nitric oxide synthase phosphorylation and expression, promoted proliferation and attenuated apoptosis of human pulmonary arterial endothelial cells *in vitro*.

Conclusion and Implications: Our findings suggest that chronic treatment with MM07 is beneficial in this animal model of pulmonary arterial hypertension by addressing disease aetiology. These data support the development of G protein-biased apelin receptor agonists with improved pharmacokinetic profiles for use in human disease.

Keywords: apelin, biased agonist, GPCR, pulmonary hypertension

Abbreviations

BMPR-II, bone morphogenetic protein receptor type II; CHX, cycloheximide; EBM-2,

endothelial basal medium 2; EGM-2,endothelial growth medium-2; FBS, foetal bovine serum; LV, left ventricle; MCT, monocrotaline; MRI, magnetic resonance imaging; PI, propidium iodide; PAECs, pulmonary artery endothelial cells; PAH, pulmonary arterial hypertension; PMVECs, pulmonary microvascular endothelial cells; rhVEGF, recombinant human vascular endothelial growth factor; RV, right ventricle, RVSP, right ventricular systolic pressure; TNFα, tumour necrosis factor α.

Introduction

The G protein-coupled apelin receptor is emerging as a novel therapeutic target for pulmonary arterial hypertension (PAH) (Yang et al., 2015) with evidence of the beneficial effect of enhancing apelin receptor signalling in PAH supported by a small number of studies from PAH patients and animal models. Expression of its endogenous ligand apelin is reduced in the circulation of patients with Group 1 pulmonary hypertension, including idiopathic PAH, PAH associated with drugs or toxins and autoimmune disease (Goetze et al., 2006; Chandra et al., 2011). In the pulmonary vasculature, pulmonary artery endothelial cells (PAECs) (Kim et al., 2013) and pulmonary microvascular endothelial cells (PMVECs) (Alastalo et al., 2011) from PAH patients express lower levels of apelin compared to cells from control donors. Mice lacking apelin develop more severe pulmonary hypertension under hypoxia (Chandra et al., 2011). Nevertheless, the apelin receptor is still present in PAH tissue (Andersen et al., 2009; Kim et al., 2013, Yang et al., 2017a) and would therefore be available as a target for exogenous agonists to replace the missing apelin. This hypothesis is substantiated by the emerging evidence that apelin may exert a range of protective effects in PAH. Apelin knockout mice develop higher right ventricular systolic pressure (RVSP), increased muscularisation of the alveolar wall arteries and more loss of pulmonary microvasculature in response to hypoxia, compared to wild-type controls (Chandra et al., 2011). Administration of the apelin peptide (Falcão-Pires et al., 2009; Alastalo et al., 2011) or other agents stimulating apelin expression (Spiekerkoetter et al., 2013; Bertero et al., 2014; Nickel et al., 2015) or downstream mediators of the apelin pathway (Kim et al., 2013) have demonstrated benefits in animal models of PAH.

Studies to date have administered the native isoforms of the apelin peptides to animal models of PAH. For example, [Pyr^{1}]apelin-13, the most predominant isoform in the human cardiovascular system (Maguire et al., 2009), was tested in monocrotaline (MCT)-induced PAH in rat (Falcão-Pires et al., 2009). As an endogenous ligand, [Pyr^{1}]apelin-13 activates both G protein and β-arrestin mediated signalling of the

apelin receptor. Activation of the β-arrestin pathway results in receptor desensitisation and internalisation, leading to loss of efficacy with chronic use (Evans et al., 2001). Importantly, β-arrestin-mediated signalling of the apelin receptor may cause stretch-induced myocardial hypertrophy and heart failure, whereas apelin-induced Gαi signalling is protective (Scimia et al., 2012). These reports suggest that minimising β-arrestin recruitment while maintaining G protein signalling would be desirable for the apelin receptor. This can be achieved by using a G protein-biased apelin receptor agonist.

We have examined signalling bias of our apelin peptide analogues designed using a combination of computational modelling and pharmacological assays, and identified MM07 as a candidate for the first synthetic biased apelin receptor agonist (Brame et al., 2015). The N terminal cyclised structure of MM07 (Figure 1A) was designed to constrain the peptide to specific conformations and protect against enzymatic degradation by non-specific aminopeptidases. Molecular dynamics simulations showed that MM07 was expected to mimic the solution conformation of apelin-13 and promote a β-turn conformation at the RPRL motif, suggested to be important for initial recognition and binding at the apelin receptor (Macaluso and Glen 2010, Brame et al., 2015). MM07 was two orders of magnitude less potent than [Pyr^1]apelin-13 in the cell-based β-arrestin and internalisation assays but was equipotent to [Pyr^1]apelin-13 in a G protein-dependent saphenous vein constriction bioassay (Brame et al., 2015). Based on these results, MM07 was found to be a G protein-biased apelin receptor agonist. In anaesthetised rats, MM07 infusion caused a greater increase in cardiac output than [Pyr^1]apelin-13 and an in vivo plasma half-life seven-fold longer than [Pyr^1]apelin-13, possibly owing to the cyclisation and also to the reduced internalisation of MM07 bound apelin receptor (Brame et al., 2015). In first-in-human experiments, MM07 was more efficacious than [Pyr^1]apelin-13 at increasing forearm blood flow and consistent with β-arrestin bias did not exhibit loss of efficacy with repeated administration (Brame et al., 2015). Additionally, both [Pyr^1]apelin-13 and MM07 reversed an established norepinephrine constriction in human hand vein (Brame et al., 2015). The aim of this proof-of-concept study was to test MM07 in the

well-established MCT-induced model of PAH. We hypothesised that MM07 would effectively attenuate MCT-induced PAH development.

Methods and Materials

Compliance with Requirements for Studies using Animals

As an animal model of PAH, rat is the preferred species relative to the mouse, because the anatomical and functional features of rat models are more reminiscent of the human disease. The MCT rat model exhibits pulmonary vascular remodelling and raised RVSP in addition to dysfunction of airways and alveoli (Colvin and Yeager, 2014). MCT rats do not develop plexiform-like lesions, however changes reported in proximal bronchovascular structures are very similar to aspects of the human condition. Moreover, the MCT model remains the only animal model of PAH that has successfully translated a therapeutic from the laboratory to the clinic, this was bosentan, the first endothelin receptor antagonist.

All rodent experiments were performed according to the local ethics committee (University of Cambridge Animal Welfare and Ethical Review Body), Home Office (UK) guidelines under the Animals (Scientific Procedures) Act 1986 Amendment Regulations (SI 2012/3039) and the ARRIVE guidelines (Kilkenny et al., 2010). All animal experiments were performed and analysed by blinded experimenters.

Experimental Rat Model of PAH

Attenuation of PAH pathogenesis by the apelin receptor agonist MM07 was tested in MCT-exposed rats using an experimental design similar to that reported by Falcão-Pires et al., 2009 (Figure 1B). Male Sprague-Dawley rats (186±2g, Charles River Laboratories) were used at a relatively young age of approximately seven weeks, which is required for the successful induction of PAH with MCT. The power calculation determining the number of animals used is as follows: $n>2\{[(Z\alpha+Z\beta)s]/\delta\}2$, where n is sample size, $Z\alpha=1.96$, $Z\beta=1.28$ for a study with 90% power and $p<0.05$ significance level, s is standard deviation, δ is minimum difference. δ is set at 20% from a sample with an SD of 10%, based on our previous data. The calculation gives $n>5.2$. The initial size of the MCT exposed groups were larger than the vehicle control group to account for possible attrition over the treatment period.

Rats were randomly allocated initially into two groups, the MCT group (n=16) were given MCT (60 mg kg^{-1} body weight) with the saline vehicle control group (n=12) receiving an equal volume of vehicle (0.9% saline) by subcutaneous injection on day 0. From day 1 to day 20, the MCT group were further divided such that 8 rats were randomised to receive daily intraperitoneal (ip) injections of MM07 (1 mg kg^{-1} body weight) and 8 to receive an equal volume of vehicle (0.9% saline) daily. Similarly, the vehicle control animals were randomised either to receive daily injections of MM07 (1 mg kg^{-1} body weight ip, n=6) or vehicle (0.9% saline ip, n=6) resulting in 4 treatment groups in total (Figure 1B). The dose of MM07 was selected based on the previously published study that found daily injections of 200 µg kg^{-1} body weight of [Pyr^{1}]apelin-13 attenuated MCT-induced PAH, and the lower affinity and potency of MM07.

The rats were accommodated under standard housing and husbandry conditions under room temperature and normoxia, in individually-ventilated cages of four rats each with wood chip bedding, under 12-hour light/ 12-hour dark cycle with *ad libitum* access to clean water and normal chow. The rats were monitored daily for signs of sickness and distress. No humane endpoint was met during the study.

Cardiac Magnetic Resonance Imaging

Magnetic resonance imaging (MRI) was carried out as previously described (Buonincontri et al., 2013) to assess cardiac performance on day 20 in a randomly selected sub-set of animals. The rats were anaesthetised with gaseous isoflurane for induction (3% in 1.5 L min^{-1} oxygen) and maintenance (2-2.5% in 1.5 L min^{-1} oxygen). A pressure sensor for respiration rate was used to monitor depth of anaesthesia, with respiration rate maintained at 45-55 breaths per minute. Body temperature was monitored using a rectal thermometer and maintained at 37°C using a flowing-water heating blanket. Prospective gating of the MRI sequences was achieved with electrocardiography monitoring using paediatric electrocardiography electrodes (3M Europe, Diegem, Belgium) on left and right forepaws. MRI was performed at 4.7 T with a Bruker BioSpec 47/40 system (Bruker Inc., Ettlingen, Germany). A birdcage coil of 12cm was used for signal excitation and animals were positioned prone over a 2cm

surface coil for signal reception. After initial localisation images, 4-chamber and 2-chamber views were obtained. Using these scans as a reference, short axis slices were acquired (FISP, TR/TE 6 ms/2.1 ms, 20-30 frames, 5 cm FOV, 256x256 matrix, 2 mm slice thickness, bandwidth 78 kHz, flip angle 20°, NEX 3), perpendicularly to both the long-axis views. Full ventricular coverage in the short axis was achieved with no slice gap with 9-10 slices. Delineation of the LV and RV, calculation of ventricular volumes and ejection fraction were performed as described using Segment v1.9 (Heiberg et al., 2010; Buonincontri et al., 2013). Owing to limitations in access to MRI facilities only 6 each of the MCT/saline and MCT/MM07 groups and 4 each of the saline and MM07 control animals were imaged, with image quality of one of the MCT animals sub-optimal to include in subsequent analysis. Group data for the MCT/Saline and MCT/MM07 groups were compared using two-tailed Student's *t*-test. The rats were allowed to recover from anaesthesia after MRI and the intraperitoneal injection for day 20 was given.

Haemodynamic Assessment by Catheterisation

On day 21, all rats were weighed and catheterised for RV hemodynamic measurements as previously described (Crosby et al., 2010; Long et al., 2015). Briefly, rats were anaesthetised with gaseous isoflurane (3% for induction, 2-2.5% for maintenance, 1.5 L min^{-1} oxygen). Body temperature was maintained at 37°C. A pressure volume catheter (SPR-869, Millar) connected to the data PowerLab 16/35 system with LabChart 5 and calibrated using the MPVS Ultra PV Unit was inserted into the RV via the right external jugular vein to measure RVSP as a surrogate for pulmonary arterial pressure. The position of the catheter was determined by the blood pressure and shape of the pressure-volume loops. The animal was allowed to stabilise for measurements. Data analysis was performed using LabChart 8 as previously described (Yang et al., 2017a). Group data were compared using one-way ANOVA with Tukey's post-test.

Analysis of Cardiac and Pulmonary Vascular Morphometry

The rats were euthanised by exsanguination, the left lung was infused with 0.8 % agarose to inflate, removed, fixed in 10% formalin (CellPath, Powys, UK), paraffin embedded and stained for smooth muscle α-actin and elastic van Gieson as described (Crosby et al., 2010; Long et al., 2015). The heart was then excised, the RV was dissected from the LV+septum and the weight ratio of these (RV compared to LV+septum), also known as the Fulton index, was determined as a measure of RV hypertrophy. In the left lung, small (diameter 25-75μm, 100 per section) pulmonary blood vessels associated with alveolar ducts were scored as completely muscular, partially muscular, or non-muscular. Statistical significance was assessed by comparing the percentage of fully muscularised vessels between groups. The wall thickness of small pulmonary arterioles (20 per section) close to terminal bronchioles was determined by measuring the average wall thickness as a percentage of average lumen diameter of the vessel using ImageJ as previously described (Yang et al., 2017a). Quantification was only performed in samples were the lungs were fully inflated, and fixation was optimal to preserve structure and to allow accurate visualisation of vascular remodelling. Therefore data for analysis were obtained from a subset of animals (n=6 each for MCT/saline and MCT/MM07 groups and n=4 each for the saline and MM07 controls). Therefore MCT/saline and MCT/MM07 data only were compared using Student's two-tailed *t*-test.

Regulation of Pulmonary Arterial Endothelial Cell Signalling

Apelin signalling is known to regulate endothelial nitric oxide synthase (eNOS), a critical enzyme that is thought to be protective in PAH, and AMP-activated protein kinase (AMPK), a regulator of energy metabolism and angiogenesis (Chandra et al., 2011; Yang et al., 2014). We have tested whether MM07 could modulate these two targets. Human PAECs (Lonza, passages 4-5) were seeded in 96 well plates (Corning) in endothelial growth medium-2 (EGM-2, Lonza) with 10% foetal bovine serum (FBS, Gibco™ Thermoscientific), allowed to attach overnight and starved for

6h in endothelial basal medium 2 (EBM-2; Lonza) with 0.5% FBS to establish baseline. The cells were treated for 15 minutes at 37°C with PBS, [Pyr^{1}]apelin-13 (100nM) or MM07 (1µM). Phosphorylated eNOS and AMPKa were detected using a previously described high throughput in-cell Western assay (Nikolic et al., 2018). The cells were fixed and permeabilised in cold 1% paraformaldehyde with 0.5% Triton-X for 20 minutes, washed and blocked in PBS with 2% bovine serum albumin (BSA, Fisher Scientific) for 2h at room temperature. A primary antibody against Serine-1177 phosphorylated eNOS (Cell Signaling Technology, 1:1000 in PBS with 2% BSA, n=11 independent experiments) or Thr-172 phosphorylated AMPKa (Cell Signaling Technology, 1:200 in PBS with 2% BSA, n=9 independent experiments) was applied for overnight incubation at 4°C. Following PBS washes, a secondary HRP-conjugated antibody (Cell Signaling Technology, 1:1000 in PBS with 2% BSA) was added for 1h incubation at room temperature. Following washes, enhanced chemiluminescence (Surmodics) measurement was performed (SpectraMax L, Molecular Devices).

In a set of separate experiments, human PAECs (Lonza, passages 4-5, n=9 independent experiments) were seeded in 6-well plates (Corning) with 10% foetal bovine serum (FBS, Gibco™ Thermoscientific), allowed to attach overnight and starved for 6h in endothelial basal medium 2 (EBM-2; Lonza) with 0.5% FBS. The cells were then treated for 24 hours at 37°C with PBS, [Pyr^{1}]apelin-13 (1µM) or MM07 (10µM). RNA extraction was performed using a Trizol® based protocol according to the manufacturer's instructions (PureLink® RNA mini kit, Life Technologies). Reverse transcription was performed with 500ng RNA according to the manufacturer's instructions (SuperScript™ IV VILO™ master mix, Invitrogen) and quantitative real-time PCR (qPCR) was performed for NOS3 (gene encoding eNOS) using 18S as internal control (AzuraView™ GreenFast qPCR Blue mix, azura genomics, Mastercycler Realplex2, Eppendorf). The primer sequences are: 18S Forward: CGGCTACCACATCCAAGGAA, Reverse: GCTGGAATTACCGCGGCT; NOS3: Forward: ATGGCGAAGCGAGTGAAG, Reverse: ACTCATCCATACACAGGACCC. Relative expression levels were calculated using the ΔΔCt method. Expression of

NOS3 mRNA was normalized to the average of the untreated control and, as is standard practice for qPCR data, expressed as relative fold change. Untreated control samples retained their individual fold change. For qPCR experiments, a one-way ANOVA with Tukey's post-test was performed to compare relative fold change between treatment groups.

Regulation of Endothelial Cell Proliferation

Apelin has been reported as a pro-proliferative and anti-apoptotic factor in endothelial cells (Alastalo et al., 2012, Kim et al., 2013). We have tested if MM07 could exert this effect in human PAECs. To study cell proliferation, human PAECs (passages 4, n=6 independent experiments) were seeded at 50,000 cell per well in 8-well chamber slides (BD Falcon) in EGM-2 with 10%FBS, allowed to attach and then starved overnight in EBM-2 with 0.5% FBS to inhibit cell division. The cells were then treated for 24h in EBM-2 with 2% FBS with PBS, [Pyr^{1}]apelin-13 (1µM), MM07 (10µM) or recombinant human vascular endothelial growth factor (rhVEGF, 20ng/mL, R&D Systems) as a positive control. The treatment media also contained 20µM 5-ethynyl-2'-deoxyuridine (EdU, part of the Click-iT® EdU Imaging Kit, Invitrogen) as a nucleoside analogue incorporated in DNA as the cells replicate. Detection of the incorporated EdU was carried out following the manufacturer's instructions. The cells were fixed with 4% paraformaldehyde with 0.5% Triton-X for 20 minutes and stained with Click-iT® EdU reaction buffer containing AlexaFluor 488 azide, copper sulphate and Click-iT® EdU buffer additive for 30 minutes at room temperature. The chambers were mounted in DAPI Vectashield medium (Vectorlabs) and imaged for blue and green fluorescence on an Olympus BX63 microscope with an EXi Blue camera (QImaging) using the cellSens software (v1.14, Oylmpus). For each cell chamber, images were taken at 10x magnification for 5 random fields based on blue DAPI fluorescence. Counting of DAPI and EdU positive cells were performed using the cellSens software with a cell area threshold to exclude cell debris and doublets applied to all images. The amount of cell proliferation was measured as the percentage of EdU positive cells to DAPI positive cells.

Rescue of Endothelial Cell Apoptosis

The effects of MM07 on endothelial cell apoptosis was tested and compared with rhVEGF using human PAECs (Lonza, passages 4-6, n=3 donors with 3 independent experiments each) as previously described (Long et al., 2015) following protocol optimisation in donor lines 1-3. Briefly, PAECs were seeded in six-well tissue culture plates at 200,000 cells/well in EGM-2 with 10% FBS and allowed to attach. On the next day, wells were washed with PBS and the media changed to either EBM-2 with 2% FBS or 10% FBS controls. MM07 (10µM) or rhVEGF (10ng/mL) were added to the wells and incubated for 18 hours. Apoptosis was induced by incubating the cells with tumour necrosis factor α (TNFα; R&D Systems, 1.5ng/mL) and cycloheximide (CHX; Sigma, 20µg/ml) for 5 hours in the experimental wells. Control wells did not receive TNFα and CHX treatment. Cells were then washed in PBS, trypsinised (Lonza), transferred into binding buffer for the apoptosis assay (Thermoscientific) and stained with anti-annexin FITC-conjugated antibody (1:2 stock dilution) and propidium iodide (PI, 20µg/mL) for 15 minutes at room temperature. Cells were filtered through 50µM filters (Sysmex Partec) and kept on ice before flow cytometry (CantoII). For each condition 10,000 events were recorded. Data analysis was performed on FlowJo v10 (FlowJo LLC, Oregon, US). $Annexin^+/PI^+$ cells were classified as 'dead', $Annexin^+/PI^-$ cells 'apoptotic' and $Annexin^-/PI^-$ as 'healthy'. Gates were adjusted such that approximately equal numbers of 'healthy' and 'apoptotic' cells occurred in the TNFα/CHX treated group as this provided a large window for either further induction or rescue of apoptosis. The raw percentage of cells in each gate were used in the data analysis. For statistical analysis, technical replicates were excluded if the apoptotic induction was less than 5%. The average induction of apoptosis of the analysed experiments was 19.53±1.76%.

Data and Statistical Analysis

Data and statistical analysis comply with the recommendations on experimental design and analysis in pharmacology. Data are expressed as mean±SEM.

Statistical analyses were conducted in GraphPad Prism 6. Post hoc tests were done only if F was significant and there was no variance in homogeneity. The number of animals in each group included for statistical tests is shown in the figure legend for that analysis. For the human PAEC assays except qPCR, as some variability in the basal amount of eNOS phosphorylation, cell proliferation and apoptotic induction was observed, as illustrated by the example of variable amounts of basal apoptotic response (Supplementary Figure 1). To minimise the confounding variability between independent experiments, a repeated measures one-way ANOVA with Dunnett's post-test was performed to compared treated groups with PBS-treated control group. For all experiments $P \leq 0.05$ was considered statistically significant.

Materials

All chemical reagents were purchased from Sigma (Poole, UK), unless otherwise stated. Human [Pyr^{1}]apelin-13 and MM07 were synthesised by Severn Biotech (Kidderminster, UK) to GLP standard using Fmoc chemistry on a solid phase support matrix to 98% purity by Maldi-TOF mass spectroscopy and HPLC analysis. Peptides were tested for sterility and demonstrated to be pyrogen free and biological activity was confirmed using a β-arrestin recruitment assay (DiscoverX, Fremont, USA) as described (Yang et al., 2017a).

Results

Cardioprotective Effects of MM07 Shown by Cardiac MRI

On day 20, changes in the appearance and motion of ventricles were detectable by non-invasive cardiac MRI, as shown in the snapshots of the heart of representative animals in the short (Figure 2A) and long (Figure 2B) axis views and in the videos (Videos 1-6). Compared to the saline-injected control rats, MCT-exposed rats developed an enlarged RV. At the end of systole, MCT-exposed rats had more residual volume in the RV compared to the controls. In early diastole, MCT exposure resulted in a distortion in the interventricular septal wall. The filling of the LV and RV appeared to be less synchronous in the MCT-exposed animals and the LV appeared to be insufficiently filled at the end of diastole. Administration of MM07 to MCT-exposed rats attenuated these structural changes, as their heart appeared to be intermediate between MCT and saline control animals. Additionally, MM07 alone did not appear to alter cardiac structure and function compared to the saline controls.

Quantitative analysis of the cardiac MRI revealed that MCT exposure resulted in an increase in RV end-diastolic and end-systolic volumes (Figure 3A-B), indicating an enlarged RV that could not contract to empty sufficiently. The compound effect of these was a reduced RV ejection fraction compared to the saline-injected control rats (Figure 3C). MCT exposure also caused LV under-filling as a consequence of reduced LV end-diastolic volume (Figure 3D), without altering LV end-systolic volume and ejection fraction (Figure 3E-F). MM07 treatment significantly attenuated MCT-induced changes in RV end-diastolic and end-systolic volumes, ejection fraction and LV end-diastolic volume. In the rats not exposed to MCT, all measured parameters with MM07 alone were comparable to the saline controls (Figure 3A-F).

MM07 Attenuated the Development of PAH in Monocrotaline Exposed Rats

Next, invasive haemodynamic measurements were carried out in isoflurane-anaesthetised rats. Compared to the saline-injected rats, RVSP was significantly

elevated in MCT-exposed rats (Figure 4A) (Table 1), indicating that these animals have developed pulmonary hypertension as expected. Compared to this group, RVSP was significantly lower in MCT-exposed rats treated with MM07, to a level that is higher than but not statistically different from the saline-injected controls. MM07 injection alone did not alter RVSP compared to the vehicle-injected group.

MM07 Attenuated Monocrotaline-Induced Right Ventricular Hypertrophy

After the animals were sacrificed, structural changes in heart ventricles were assessed. Compared to the controls, the Fulton index were significantly increased in in MCT-exposed rats, indicating the development of RV hypertrophy (Figure 4B) (Table 1). This structural change of the RV was significantly attenuated by MM07 administration. However, MM07 did not completely abolish the development of RV hypertrophy resulting from MCT. MM07 injection alone did not alter the Fulton index compared to the saline controls.

MM07 Attenuated Monocrotaline-Induced Pulmonary Vascular Remodelling

In order to determine the effect of MM07 on the pathogenesis of PAH, morphometry of pulmonary arterioles was examined and the extent of vascular remodelling was scored. Representative photomicrographs of rat lung sections with smooth muscle actin and van Giesen's staining are shown in Figure 5. As expected, MCT injection increased the percentage of fully muscularised small vessels (Figure 6A) and the wall thickness of small to medium-sized arterioles (Figure 6B) (Table 1). MCT-induced vascular remodelling was attenuated by MM07 administration, as the proportion of fully muscularised small vessels and the arteriolar wall thickness were significantly reduced. The extent of small vessel muscularisation and arteriolar wall thickness was similar in saline and MM07-injected control groups.

MM07 Activates Endothelial Nitric Oxide Synthase and AMP-Activated Protein Kinase

In order to investigate the potential mechanisms underlying the benefit of MM07 in

MCT-induced PAH, we have tested the effect of MM07 on protective signalling in PAECs known to be activated by apelin signalling. Knockdown of apelin expression reduces the phosphorylation and activation of eNOS and AMPK in PAECs (Chandra et al., 2011). Human PAECs were stimulated acutely with [Pyr^{1}]apelin-13 or MM07. Both ligands significantly increased phosphorylation of eNOS (Figure 7A) and AMPKa (Figure 7B), compared to control cells. Stimulation of PAECs with [Pyr^{1}]apelin-13 or MM07 also increased the mRNA levels of eNOS (NOS3 gene) (Figure 7C).

MM07 Promoted Proliferation of Pulmonary Arterial Endothelial Cells

Next, we examined the functional effect of MM07 on endothelial cell homeostasis. Previous studies have shown that apelin induced proliferation of PAECs and PMVECs (Alastalo et al., 2011, Kim et al., 2013). We have stimulated human PAECs with ligands and measured cell proliferation using a DNA replication-based assay. Significantly more EdU incorporation was induced by the positive control treatment, rhVEGF, compared to untreated controls. Similarly, both [Pyr^{1}]apelin-13 and MM07 significantly resulted in significantly higher proportion of proliferating cells (Figure 8A for representative images and 8B for inter-group comparisons).

MM07 Exerted Anti-Apoptotic Effects on Pulmonary Arterial Endothelial Cells

Apelin has been reported to have anti-apoptotic roles on endothelial cells in the pulmonary circulation (Alastalo et al., 2011; Kim et al., 2013). The effect of MM07 on apoptosis of primary human PAECs was investigated using donor cell lines. Treatment with TNFα/CHX resulted in a significant increase in Annexin^{+}/PI^{-} staining (19.5%). rhVEGF pre-treatment for 18 hours significantly attenuated this apoptotic induction (11.6%) as did MM07 (4.5%) (Figure 9). In control experiments, EBM-2 2% FBS control (serum and growth factor starved) was compared to a healthy control (EGM-2 10% FBS) and the extent of rhVEGF and MM07 rescue on serum and growth factor starvation assessed. Serum and growth factor starvation resulted in a significant induction of Annexin^{+}/PI^{-} staining (9.3%) which was almost wholly rescued

by 18 hours of rhVEGF pre-treatment (8.9%). However, MM07 displayed no rescue from serum and growth factor starvation (Supplementary Figure 2).

Discussion and Conclusions

This is the first study of an apelin receptor biased agonist in an animal model of disease. Our results showed that MM07 attenuated the elevation of RVSP, RV hypertrophy, cardiac dysfunction and pulmonary vascular remodelling induced by MCT. MM07 also conferred pro-proliferative and anti-apoptotic effects on human PAECs *in vitro*. Our findings suggest that G protein-biased agonism of the apelin receptor has potential beneficial effects in PAH, indicating that the apelin receptor is a therapeutic target tractable to biased agonism.

The goal of supplying exogenous apelin receptor agonist in PAH is to replace the missing endogenous peptide. The reduction in apelin expression has been shown to result from the dysfunction of bone morphogenetic protein receptor type II (BMPR-II) (Alastalo et al., 2011) which is the most frequently mutated gene in familial and sporadic PAH (Machado et al., 2015) and a critical component in a pathway central to PAH pathogenesis (Morrell et al., 2015). It has been reported that apelin is a transcriptional target of BMPR-II, mediated by the miR-130/301 family and PPARγ in pulmonary vascular endothelial cells (Alastalo et al., 2011; Bertero et al., 2014). Furthermore, apelin expression in the RV is decreased in the MCT (Falcão-Pires et al., 2009) and Sugen 5416+hypoxia-induced (Drake et al., 2011; Frump et al., 2015) rat models of PAH. Importantly, apelin levels are found to be correlated with contractile and diastolic function of the RV in the Sugen+hypoxia model (Neto-Neves et al., 2017). Interestingly, elabela/toddler, the second endogenous ligand of the apelin receptor encoded by *APELA* gene, is also reduced in cardiopulmonary tissues from PAH patients and animal models (Yang et al., 2017a). In an early study of particular interest, the apelin peptide was tested in MCT-induced PAH (Falcão-Pires et al., 2009). The apelin signalling pathway is also implicated in pulmonary veno-occlusive disease (Lathen et al., 2014) and chronic thromboembolic pulmonary hypertension (Miao et al., 2017). As expected, agents that activate apelin expression or act as downstream effectors of apelin signalling have demonstrated beneficial effects in PAH animal models (Kim et al., 2013; Spiekerkoetter et al., 2013; Bertero et al., 2014; Nickel et al.,

2015).

One caveat may limit the therapeutic efficacy and clinical development of native apelin peptides. As a G protein-coupled receptor, the ligand-activated apelin receptor is phosphorylated by G protein-coupled receptor kinases and β-arrestin is recruited to the receptor. This switches off G protein-mediated signalling, triggers receptor desensitisation, internalisation and removal of the bound apelin ligand, leading to loss of efficacy with chronic administration of the peptide (Evans et al., 2001; Violin and Lefkowitz 2007; Rajagopal et al., 2010). Importantly, β-arrestin-mediated signalling is also involved in an apelin-independent stretch-sensitive function of the apelin receptor and may cause myocardial hypertrophy and heart failure, whereas apelin-induced $G_{\alpha i}$ signalling is protective (Scimia et al., 2012). This need to selectively or preferentially activate a subset of downstream signalling pathways forms the rationale to investigate signalling bias and develop G protein-biased agonists of the apelin receptor. Using a number of in vitro screening assays, our lab have discovered MM07, the first apelin analogue peptide acting as a G protein-biased agonist of the apelin receptor (Brame et al., 2015).

Having demonstrated the activity of MM07 *in vivo* under normal physiological conditions (Brame et al., 2015), we tested this peptide, or more generally the concept of G protein-biased agonism of the apelin receptor, in a disease model. The current study used an experimental design with the same dose of MCT and time course as Falcão-Pires et al., 2009, in order to verify if MM07 could attenuate the development of PAH. In this previous three-week experiment, rats injected with 60mgkg^{-1} MCT were treated with intraperitoneal injections of the predominant endogenous apelin peptide, [Pyr^{1}]apelin-13, at a dose of 200μgkg^{-1} per day. The authors reported that [Pyr^{1}]apelin-13 ameliorated the elevation in RVSP and development of RV hypertrophy, but failed to attenuate the thickening of pulmonary arterioles (Falcão-Pires et al., 2009). Owing to the lower receptor binding affinity and potency of MM07 compared to [Pyr^{1}]apelin-13 (Brame et al., 2015), a higher dose of MM07 (1mgkg^{-1} per day) was used compared to the previous study with [Pyr^{1}]apelin-13 (200μgkg^{-1} per day in Falcão-Pires et al., 2009).

The cardiac MRI showed that MCT caused an enlargement of the RV and systolic dysfunction, indicating the RV failed to match the increased afterload due to increased pulmonary vascular resistance, consistent with previous reports (Porvasnik et al., 2010, Redout et al., 2010). The combined effect of a lowered RV output, compression of the LV due to RV enlargement and the leftward septal displacement led to under filling of the LV, as shown by the reduced LV volume at end-diastole (Gan et al., 2006). Importantly, MM07 attenuated the detrimental effects of MCT by limiting the enlargement of the RV and improving its ejective function which in turn alleviated under-filling of the LV. In healthy control animals, MM07 did not significantly alter any of these parameters, suggesting that its actions can only be revealed upon injury with MCT and does not affect the normal physiological function. Previous studies have proposed possible explanations for the observed benefits of MM07. Apelin receptor signalling is known to increase cardiac contractility and output (Szokodi et al., 2002; Maguire et al., 2009; Brame et al., 2015), possibly by activating myosin light chain kinase to increase myofilament calcium sensitivity (Perjés et al., 2014) and by a positive lusitropic effect (Peyronnet et al., 2017), so the enhanced cardiac performance does not require an increase in oxygen consumption (Charo et al., 2009). MM07-induced haemodynamic improvement was confirmed by invasive right heart catheterisation. MM07-injected rats were shown to have significantly lower RVSP in response to MCT exposure compared to those not treated with MM07. This is unlikely to be caused by an acute vasodilatory effect of MM07, as the compound was not injected on the day of catheterisation. In agreement, chronic administration of the native apelin peptide has been reported to reduce RVSP in mouse and rat models of PAH (Falcão-Pires et al., 2009; Alastalo et al., 2011). Importantly, MCT-induced RV hypertrophy was less pronounced in MM07-treated rats, consistent with the previous study showing that apelin receptor ligand-activated $G_{\alpha i}$ protein signalling protected against cardiac hypertrophy and failure (Scimia et al., 2012). Taken together, our physiological results have demonstrated a protective of MM07 against MCT- induced cardiac dysfunction.

While the signalling pathways activated by the apelin receptor are not fully

characterized, previous studies have shown that eNOS expression and phosphorylation is reduced with apelin knockdown and in apelin knockout animals (Chandra, et al., 2011), but eNOS phosphorylation can be induced by [Pyr^{1}]apelin-13 and elabela/toddler (Yang et al., 2017a). We have found that MM07 could also induce eNOS phosphorylation acutely and then increase eNOS expression in human PAECs. The important role of eNOS is demonstrated by the increased susceptibility to hypoxia-induced pulmonary hypertension in eNOS deficient mice (Fagan et al., 1999) and by the therapeutic benefit of eNOS gene transfer in MCT-exposed rats (Zhao et al., 2006). Importantly, eNOS functions beyond generating a vasodilator, as eNOS gene transfer restored the microvascular loss in the MCT model (Zhao et al., 2006). AMPK has been reported to mediate the pro-angiogenic effects of apelin and activation of AMPK has beneficial effect in PAH animal models (Chandra, et al., 2011; Yang et al., 2014). We have found that MM07 could increase the phosphorylation of AMPKa in endothelial cells. There are other potential mechanisms for the beneficial effects of MM07, it is clear that apelin receptor signalling regulates multiple effector pathways and cell types in the pulmonary vasculature. For example, apelin was reported to induce the endothelial ATPase CD39 and limit the emergence of apoptosis-resistant PAECs (Helenius et al., 2015), possibly at a later stage of PAH pathogenesis. Moreover, it has been reported that apelin regulates myocyte enhancer factor 2, which in turn activates miR-424/miR-503 and genes contributing to endothelial homeostasis. This axis also inhibits the expression of fibroblast growth factor 2 and its receptor and thus exerts anti-proliferative effects on pulmonary arterial smooth muscle cells (Alastalo et al., 2011; Kim et al., 2013; Helenius et al., 2015; Kim et al., 2015). Further experiments, possibly using a co-culture system, are required to understand how G protein-biased apelin signalling in endothelial cell may impact the homeostasis of smooth muscle cells.

It has been suggested that the benefits of apelin may extend beyond its acute vasodilatory and positive inotropic activities, as apelin regulates the homeostasis of pulmonary vascular cells. Conversely, deficiency of apelin may contribute to the imbalance between proliferation and apoptosis of these cells, leading to pathological

vascular remodelling, which is the ultimate cause of PAH (Andersen et al., 2011; Yang et al., 2015). In the current study, MM07 demonstrated disease modification as it attenuated pulmonary vascular remodelling in terms of arteriolar muscularisation and wall thickening, thereby mitigating the key driving feature in the pathogenesis of PAH (Rabinovitch 2012; Morrell et al., 2016). Endothelial apoptosis is thought to initiate PAH and contribute to the loss of microvasculature in human disease and animal models (Wilson et al., 1992; Rabinovitch 2012). In this study, we have investigated the effect of MM07 on the homeostasis of PAECs, in order to understand the mechanism underlying its protective effects on vascular remodelling. Apelin has been reported to promote survival of pulmonary vascular endothelial cells (Alastalo et al., 2011; Kim et al., 2013). We used an EdU incorporation assay to measure cell proliferation, which has the advantage of not being confounded by the metabolic state of the cell, as it measures DNA synthesis directly. We found that MM07 promoted PAEC proliferation in 24h, as did [Pyr^{1}]apelin-13. To test the ability of MM07 to rescue endothelial apoptosis, we utilised a previously published apoptosis assay using TNFα/CHX to induce apoptosis in healthy human PAECs (Long et al., 2015). Under usual conditions TNFα prevents apoptosis of endothelial cells through activation of the NF-κB pathway, however, in conditions of global protein synthesis suppression, such as produced by concurrent application of CHX, apoptosis is induced through TNF-R1 leading to JNK phosphorylation. In our experiments, MM07, reduced apoptosis of healthy human PAECs induced by TNFα/CHX, demonstrating prevention of endothelial damage *in vitro*. Interestingly, MM07 did not rescue endothelial damage caused by growth factor and serum starvation, a less severe treatment than TNFα/CHX, suggesting it may be more suitable in early disease where high levels of endothelial damage are thought to be critical drivers of disease development. We acknowledge that PMVECs may be more reminiscent of endothelium from the small pulmonary vessels than PAECs. However, the pro-proliferative and anti-apoptotic effect of native apelin peptide have been reported in both normal PAECs and PMVECs (Alastalo et al., 2011; Kim et al., 2013), and even in endothelial cells from other vascular beds or organisms (summarised in Pitkin et al., 2011). Overall, our finding

provides a mechanism and supports apelin mimetics as important in treating disease aetiology itself rather than simply relying on vasodilatation, as is the case with current therapeutics.

Recent studies have generated more insight on the apelin receptor structure (Ma et al., 2017), apelin degradative pathways (Murza et al., 2014; McKinnie et al., 2016; Yang et al., 2017b), antagonists (Le Gonidec et al., 2017) and more peptide biased agonists of the apelin receptor (Ceraudo et al., 2014; McAnally et al., 2017; Murza et al., 2017), providing new tools to further investigate biased agonism of the apelin receptor. One pharmacokinetic property that distinguishes MM07 from [Pyr^{1}]apelin-13 is stability. Although still relatively short at under 20 minutes, MM07 has a significantly longer *in vivo* plasma half-life than [Pyr^{1}]apelin-13 (Brame et al., 2015), which may be a consequence of its N terminal cyclisation and/or reduced removal due to receptor internalisation. This may have enabled MM07 to produce greater target cover compared to [Pyr^{1}]apelin-13 with each daily injection. Our previous human study has shown that the magnitude of vascular response drops with repeated dosing of [Pyr^{1}]apelin-13 owing to receptor desensitisation, but not with MM07 (Brame et al., 2015). This phenomenon may also contribute to the benefit of MM07 observed in the current chronic study. Building on the efficacy of MM07, novel biased apelin receptor agonists with higher binding affinity, higher potency in G protein signalling, more G protein bias and even better stability, such as the small molecule CMF-019 (Read et al., 2016), could be tested in PAH animal models in future studies. As G protein-biased agonism of the apelin receptor was shown to be safe in chronic use, further studies may be able to reduce the number of animals in the agonist-only control group.

This study has demonstrated that a G protein-biased agonist of the apelin receptor could attenuate the development of MCT-induced PAH, which is an acute model of moderate severity. In future studies, this concept could be validated in the Sugen5416 and chronic hypoxia-induced model of PAH which exhibits more severe pulmonary vascular remodelling (Stenmark et al., 2009). More importantly what is required to corroborate the data we have obtained with MM07 in the MCT prevention model is testing of an apelin G protein-biased agonist in a more clinically relevant

reversal model of PAH. This may require the development of apelin agonists with improved pharmacokinetic properties to allow maintained target exposure from once a day administration beyond that which is likely achieved with the relatively short lived peptide MM07.

In conclusion, this proof-of-principle study demonstrated the effectiveness of MM07, a G protein-biased agonist of the apelin receptor, in attenuating the development of MCT-induced PAH. In addition to reducing the elevation of RVSP and hypertrophy as previously shown with [Pyr^{1}]apelin-13, MM07 also attenuated functional changes of the heart and vascular remodelling in the lung. At the cellular level, MM07 acts as a pro-proliferative and anti-apoptotic factor that activates beneficial signalling in endothelial cells. By selectively activating downstream pathways, biased agonists have been shown to be equally effective as the native unbiased agonist with extra benefits owing to the differential signalling. This is illustrated by the G protein-biased agonists of the μ-opioid receptor, TRV130 and PZM21, which produced greater pain relief than morphine with reduced β arrestin-mediated respiratory depression (Manglik et al., 2016; Viscusi et al., 2016). The results from the current study suggest that biased agonism may also be exploited in the treatment of PAH.

References

Alastalo TP, Li M, Perez Vde J, Pham D, Sawada H, Wang JK et al (2011). Disruption of PPAR gamma/beta-catenin-mediated regulation of apelin impairs BMP-induced mouse and human pulmonary arterial EC survival. *J Clin Invest* **121**:3735-3746.

Andersen CU, Markvardsen LH, Hilberg O, Simonsen U (2009). Pulmonary apelin levels and effects in rats with hypoxic pulmonary hypertension. *Respir Med* **103**:1663-1671.

Andersen CU, Hilberg O, Mellemkjaer S, Nielsen-Kudsk JE, Simonsen U (2011). Apelin and pulmonary hypertension. *Pulm Circ* **1**:334-346.

Bertero T, Lu Y, Annis S, Hale A, Bhat B, Saggar R et al (2014). Systems-level regulation of microRNA networks by miR-130/301 promotes pulmonary hypertension. *J Clin Invest* **124**:3514-3528.

Brame AL, Maguire JJ, Yang P, Dyson A, Torella R, Cheriyan J et al (2015). Design, characterization, and first-in-human study of the vascular actions of a novel biased apelin receptor agonist. *Hypertension* **65**:834-840.

Buonincontri G, Methner C, Carpenter TA, Hawkes RC, Sawiak SJ, Krieg T (2013). MRI and PET in mouse models of myocardial infarction. *J Vis Exp* 2013:e50806.

Ceraudo E, Galanth C, Carpentier E, Banegas-Font I, Schonegge AM, Alvear-Perez R et al (2014) Biased signalling favoring Gi over beta-arrestin promoted by an apelin fragment lacking the C-terminal phenylalanine. *J Biol Chem* **289**:24599-24610.

Chandra SM, Razavi H, Kim J, Agrawal R, Kundu RK, de Jesus Perez V et al (2011). Disruption of the apelin-APJ system worsens hypoxia-induced pulmonary hypertension. *Arterioscler Thromb Vasc Biol* **31**:814-820.

Charo DN, Ho M, Fajardo G, Kawana M, Kundu RK, Sheikh AY et al (2009). Endogenous regulation of cardiovascular function by apelin-APJ. *Am J Physiol*

Heart Circ Physiol **297**: H1904-H1913.

Colvin KL, Yeager ME (2014). Animal models of pulmonary hypertension: Matching disease mechanisms to etiology of the human disease. *J Pulm Respir Med* **4**:198.

Crosby A, Jones FM, Southwood M, Stewart S, Schermuly R, Butrous G et al (2010). Pulmonary vascular remodelling correlates with lung eggs and cytokines in murine schistosomiasis. *Am J Respir Crit Care Med* **181**:279-288.

Drake JI, Bogaard HJ, Mizuno S, Clifton B, Xie B, Gao Y et al (2011). Molecular signature of a right heart failure program in chronic severe pulmonary hypertension. *Am J Respir Cell Mol Biol* **45**:1239-1247.

Evans NA, Groarke DA, Warrack J, Greenwood CJ, Dodgson K, Milligan G et al (2001). Visualizing differences in ligand-induced beta-arrestin-GFP interactions and trafficking between three recently characterized G protein-coupled receptors. *J Neurochem* 77:476-485.

Fagan KA, Fouty BW, Tyler RC, Morris KG Jr, Hepler LK, Sato K et al (1999). The pulmonary circulation of homozygous or heterozygous eNOS-null mice is hyperresponsive to mild hypoxia. *J Clin Invest* **103**:291–299

Falcão-Pires I, Goncalves N, Henriques-Coelho T, Moreira-Goncalves D, Roncon-Albuquerque R Jr, Leite-Moreira AF (2009). Apelin decreases myocardial injury and improves right ventricular function in monocrotaline-induced pulmonary hypertension. *Am J Physiol Heart Circ Physiol* **296**:H2007-2014.

Frump AL, Goss KN, Vayl A, Albrecht M, Fisher A, Tursunova R et al (2015). Estradiol improves right ventricular function in rats with severe angioproliferative pulmonary hypertension: effects of endogenous and exogenous sex hormones. *Am J Physiol Lung Cell Mol Physiol* **308**:L873-390.

Gan C, Lankhaar JW, Marcus JT, Westerhof N, Marques KM, Bronzwaer JG et al (2006). Impaired left ventricular filling due to right-to-left ventricular interaction in patients with pulmonary arterial hypertension. *Am J Physiol Heart Circ Physiol* **290**:H1528-1533.

Goetze JP, Rehfeld JF, Carlsen J, Videbaek R, Andersen CB, Boesgaard S et al (2006) Apelin: a new plasma marker of cardiopulmonary disease. *Regul Pept* **133**:134-138.

Heiberg E, Sjogren J, Ugander M, Carlsson M, Engblom H, Arheden H (2010). Design and validation of Segment--freely available software for cardiovascular image analysis. *BMC Med Imaging* **10**:1.

Helenius MH, Vattulainen S, Orcholski M, Aho J, Komulainen A, Taimen P et al (2015). Suppression of endothelial CD39/ENTPD1 is associated with pulmonary vascular remodelling in pulmonary arterial hypertension. *Am J Physiol Lung Cell Mol Physiol* **308**:L1046-1057.

Kilkenny C, Browne WJ, Cuthill IC, Emerson M, Altman DG (2010). Improving Bioscience Research Reporting: The ARRIVE Guidelines for Reporting Animal Research. *PLoS Biol* **8(6)**: e1000412.

Kim J, Kang Y, Kojima Y, Lighthouse JK, Hu X, Aldred MA et al (2013). An endothelial apelin-FGF link mediated by miR-424 and miR-503 is disrupted in pulmonary arterial hypertension. *Nat Med* **19**:74-82.

Kim J, Hwangbo C, Hu X, Kang Y, Papangeli I, Mehrotra D et al (2015). Restoration of impaired endothelial myocyte enhancer factor 2 function rescues pulmonary arterial hypertension. *Circulation* **131**:190-199

Lathen C, Zhang Y, Chow J, Singh M, Lin G, Nigam V (2014). ERG-APLNR axis controls pulmonary venule endothelial proliferation in pulmonary veno-occlusive disease. *Circulation* **130**:1179-1191.

Le Gonidec S, Chaves-Almagro C, Bai Y, Kang HJ, Smith A, Wanecq E (2017). Protamine is an antagonist of apelin receptor, and its activity is reversed by heparin. *FASEB J* **31**:2507-2519.

Long L, Ormiston ML, Yang X, Southwood M, Graf S, Machado RD et al (2015). Selective enhancement of endothelial BMPR-II with BMP9 reverses pulmonary arterial hypertension. *Nat Med* **21**:777-785.

Ma Y, Yue Y, Ma Y, Zhang Q, Zhou Q, Song Y et al (2017). Structural basis for apelin control of the human apelin receptor. *Structure* **25**:858-866.

Macaluso NJ, Glen RC (2010). Exploring the 'RPRL' motif of apelin-13 through molecular simulation and biological evaluation of cyclic peptide analogues. *ChemMedChem* **5**:1247-1253.

Machado RD, Southgate L, Eichstaedt CA, Aldred MA, Austin ED, Best DH et al (2015). Pulmonary arterial hypertension: a current perspective on established and emerging molecular genetic defects. *Hum Mutat* **36**:1113-27.

Maguire JJ, Kleinz MJ, Pitkin SL, Davenport AP (2009). [Pyr1]apelin-13 identified as the predominant apelin isoform in the human heart: vasoactive mechanisms and inotropic action in disease. *Hypertension* **54**:598-604.

Manglik A, Lin H, Aryal DK, McCorvy JD, Dengler D, Corder G et al (2016). Structure-based discovery of opioid analgesics with reduced side effects. *Nature* **537**:185-190.

Masri B, Lahlou H, Mazarguil H, Knibiehler B, Audigier Y (2002). Apelin (65-77) activates extracellular signal-regulated kinases via a PTX-sensitive G protein. *Biochem Biophys Res Commun* **290**:539-545.

McAnally D, Siddiquee K, Sharir H, Qi F, Phatak S, Li JL et al (2017). A Systematic Approach to Identify Biased Agonists of the Apelin Receptor through High-Throughput Screening. *SLAS Discov* **22**:867-878.

McKinnie SM, Fischer C, Tran KM, Wang W, Mosquera F, Oudit et al (2016). The Metalloprotease Neprilysin Degrades and Inactivates Apelin Peptides. *Chembiochem* **17**:1495-1498.

Miao R, Wang Y, Wan J, Leng D, Gong J, Li J et al (2017). Microarray analysis and detection of microRNAs associated with chronic thromboembolic pulmonary hypertension. *Biomed Res Int* 2017:8529796.

Morrell NW, Bloch DB, ten Dijke P, Goumans MJ, Hata A, Smith J et al (2016). Targeting BMP signalling in cardiovascular disease and anaemia. *Nat Rev*

Cardiol **13**:106-120.

Murza A, Belleville K, Longpre JM, Sarret P, Marsault E (2014). Stability and degradation patterns of chemically modified analogs of apelin-13 in plasma and cerebrospinal fluid. *Biopolymers* **102**:297-303.

Murza A, Sainsily X, Côté J, Bruneau-Cossette L, Besserer-Offroy É, Longpré JM et al (2017). Structure-activity relationship of novel macrocyclic biased apelin receptor agonists. *Org Biomol Chem* **15**:449-458.

Neto-Neves EM, Frump AL, Vayl A, Kline JA, Lahm T (2017). Isolated heart model demonstrates evidence of contractile and diastolic dysfunction in right ventricles from rats with sugen/hypoxia-induced pulmonary hypertension*. Physiol Rep* **5**: e13438

Nickel NP, Spiekerkoetter E, Gu M, Li CG, Li H, Kaschwich M et al (2015). Elafin reverses pulmonary hypertension via caveolin-1-dependent bone morphogenetic protein signaling. *Am J Respir Crit Care Med* **191**:1273-1286.

Nikolic I, Yung LM, Yang P, Malhotra R, Paskin-Flerlage SD, Dinter T et al (2018). Bone Morphogenetic Protein 9 is a Mechanistic Biomarker of Portopulmonary Hypertension. A*m J Respir Crit Care Med* in press.

Perjes A, Skoumal R, Tenhunen O, Konyi A, Simon M, Horvath IG et al (2014). Apelin increases cardiac contractility via protein kinase Cepsilon- and extracellular signal-regulated kinase-dependent mechanisms. *PloS one* **9**:e93473.

Peyronnet R, Bollensdorff C, Capel RA, Rog-Zielinska EA, Woods CE, Charo DN et al (2017). Load-dependent effects of apelin on murine cardiomyocytes. *Prog Biophys Mol Biol* **130**:333-343.

Pitkin SL, Maguire JJ, Bonner TI, Davenport AP (2011). International Union of Basic and Clinical Pharmacology. LXXIV. Apelin receptor nomenclature, distribution, pharmacology, and function. *Pharmacol Rev* **62**:331-342.

Porvasnik SL, Germain S, Embury J, Gannon KS, Jacques V, Murray J et al

(2010). PRX-08066, a novel 5-hydroxytryptamine receptor 2B antagonist, reduces monocrotaline-induced pulmonary arterial hypertension and right ventricular hypertrophy in rats. *J Pharmacol Exp Ther* **334**:364-372

Rabinovitch M (2012). Molecular pathogenesis of pulmonary arterial hypertension. *J Clin Invest* **122**:4306-4313.

Rajagopal S, Rajagopal K, Lefkowitz RJ (2010). Teaching old receptors new tricks: biasing seven-transmembrane receptors. *Nat Rev Drug Discov* **9**:373-386.

Read C, Fitzpatrick CM, Yang P, Kuc RE, Maguire JJ, Glen RC et al (2016). Cardiac action of the first G protein biased small molecule apelin agonist. *Biochem Pharmacol* **116**:63-72.

Redout EM, van der Toorn A, Zuidwijk MJ, van de Kolk CW, van Echteld CJ, Musters RJ et al (2010). Antioxidant treatment attenuates pulmonary arterial hypertension-induced heart failure. *Am J Physiol Heart Circ Physiol* **298**:H1038-1047.

Scimia MC, Hurtado C, Ray S, Metzler S, Wei K, Wang J et al (2012). APJ acts as a dual receptor in cardiac hypertrophy. *Nature* **488**:394-398.

Spiekerkoetter E, Tian X, Cai J, Hopper RK, Sudheendra D, Li CG et al (2013). FK506 activates BMPR2, rescues endothelial dysfunction, and reverses pulmonary hypertension. *J Clin Invest* **123**:3600-3613.

Stenmark KR, Meyrick B, Galie N, Mooi WJ, McMurtry IF (2009). Animal models of pulmonary arterial hypertension: the hope for etiological discovery and pharmacological cure. *Am J Physiol Lung Cell Mol Physiol* **297**:L1013-32.

Szokodi I, Tavi P, Foldes G, Voutilainen-Myllyla S, Ilves M, Tokola H et al (2002). Apelin, the novel endogenous ligand of the orphan receptor APJ, regulates cardiac contractility. *Circ Res* **91**:434-440.

Wilson DW, Segall HJ, Pan LC, Lamé MW, Estep JE, Morin D (1992). Mechanisms and pathology of monocrotaline pulmonary toxicity. *Crit Rev Toxicol* **22**:307–325.

Violin JD, Lefkowitz RJ (2007). Beta-arrestin-biased ligands at seven-transmembrane receptors. *Trends Pharmacol Sci* **28**:416-422.

Viscusi ER, Webster L, Kuss M, Daniels S, Bolognese JA, Zuckerman S et al (2016). A randomized, phase 2 study investigating TRV130, a biased ligand of the mu-opioid receptor, for the intravenous treatment of acute pain. *Pain* **157**:264-272.

Yang P, Maguire JJ, Davenport AP (2015). Apelin, Elabela/Toddler, and biased agonists as novel therapeutic agents in the cardiovascular system. *Trends Pharmacol Sci* **36**:560-567.

Yang P, Read C, Kuc RE, Buonincontri G, Southwood M, Torella R et al (2017a). Elabela/toddler is an endogenous agonist of the apelin APJ receptor in the adult cardiovascular system, and exogenous administration of the peptide compensates for the downregulation of its expression in pulmonary arterial hypertension. *Circulation* **135**:1160-1173.

Yang P, Kuc RE, Brame AL, Dyson A, Singer M, Glen RC et al (2017). [Pyr^{1}]Apelin-13$_{(1\text{-}12)}$ is a biologically active ACE2 metabolite of the endogenous cardiovascular peptide [Pyr^{1}]Apelin-13. *Front Neurosci* **11**:92.

Yang X, Zhu W, Zhang P, Chen K, Zhao L, Li J et al (2014). Apelin-13 stimulates angiogenesis by promoting cross‐talk between AMP-activated protein kinase and Akt signaling in myocardial microvascular endothelial cells. *Mol Med Rep* **9**:1590-1596.

Zhao YD, Courtman DW, Ng DS, Robb MJ, Deng YP, Trogadis J et al (2006). Microvascular regeneration in established pulmonary hypertension by angiogenic gene transfer. *Am J Respir Cell Mol Biol* **35**:182–189.

Table 1. MM07 attenuated MCT-induced changes in RVSP, RV hypertrophy and pulmonary vascular remodelling

	MCT	MCT+MM07	MM07	Control
n number	8	8	6	6
Body weight (g)	303±8	295±4	343±9	343±2
RVSP (mmHg)	50.6±5.9 †	28.2±2.2 ‡	22.9±1.7	21.9±1.9
Systolic pressure (mmHg)	105.5±2.0	105.2±1.2	108.2±3.7	104.5±1.6
Diastolic pressure (mmHg)	76.5±2.5	76.4±0.9	77.0±2.0	77.3±1.2
Heart rate (bpm)	363±6	365±7	368±15	361±15
RV weight (g)	0.27±0.02	0.23±0.02	0.16±0.01	0.16±0.01
LV+S weight (g)	0.67±0.02	0.70±0.02	0.71±0.02	0.74±0.01
RV/(LV+S)	0.40±0.02 †	0.33±0.03 †‡	0.22±0.02	0.21±0.01
Fully muscularised vessels	32±1% †	24±2% †‡	15±1%	14±1%
Vessel wall thickness	21±1% †	16±1% †‡	10±1%	10±1%

† Significantly different versus saline control, ‡ significantly different versus MCT-exposed rats, as determined by one-way ANOVA with Tukey's post-test. Data are expressed as mean±sem. $P \leq 0.05$ is considered statistically significant.

Figure Legends

Figure 1: (A) Amino acid sequences of MM07 aligned with the sequence of the endogenous agonist [Pyr^{1}]apelin-13. Disulphide bridge is shown as yellow lines, hydrophobic amino acids shown in green, uncharged polar amino acids in pink, basic amino acids in blue with pyroglutamate in red. (B) Experimental design of the MM07-MCT study. Rats were given MCT (60 mg kg^{-1}) or vehicle on day 0 and daily injections of MM07 (1 mg kg^{-1}) or vehicle from day 1 to day 20. Cardiac MRI was conducted on day 20 and closed-chest catheterisation was performed on day 21. The animals were then euthanized to tissue collection. BW, body weight; sc, subcutaneous; ip, intraperitoneal.

Figure 2: MRI of rat hearts in the MM07-MCT study. Representative snapshots of cardiac MRI scans at end-systolic, early diastolic and end-diastolic points from MCT, MCT+MM07, MM07 and saline injected rats. (A) Short axis views with the RV on the left side. (B) Long axis views with the RV at the bottom side. Red arrows are drawn to show the point of septal wall bowing at early diastole.

Figure 3: Quantitative analysis of cardiac MRI. (A) MM07 attenuated MCT-induced increase in RV end-diastolic volume. (B) MM07 attenuated MCT-induced increase in RV end-systolic volume. (C) MM07 attenuated MCT-induced decrease in RV ejection fraction. (D) MM07 attenuated MCT-induced decrease in LV end-diastolic volume. (E) MCT and MM07 did not alter LV end-systolic volume. (F) MCT and MM07 did not alter LV ejection fraction. (MCT n=7, MCT-MM07 n=8, MM07 n=4, saline n=4). *P≤0.05, determined by Student's two-tailed *t*-test. Data are expressed as mean±sem. EDV, end-diastolic volume; ESV, end-systolic volume; EF, ejection fraction.

Figure 4: Attenuation of MCT-induced PAH by MM07 administration. (A) MM07 attenuated MCT-induced elevation in RVSP. (B) MM07 attenuated MCT-induced RV

hypertrophy, measured as RV/(LV+S), or Fulton index (MCT n=8, MCT-MM07 n=8, MM07 n=6, saline n=6). *P≤0.05, ns not significant, as determined by one-way ANOVA with Tukey's post-test. Data are expressed as mean±sem.

Figure 5: Immunohistological visualization of remodelling of pulmonary arterioles, shown as a vessel close to a terminal bronchiole, using α-smooth muscle actin (brown colour A-D) and van Gieson's stain (E-H) in sections of lung from (A, E) MCT, (B, F) MCT+MM07, (C, G) MM07 and (D, H) saline control rats (scale bars=75μm).

Figure 6: Attenuation of MCT-induced pulmonary vascular remodelling by MM07 administration (MCT n=5, MCT-MM07 n=6, MM07 n=4, saline n=4), measured as (A) proportion of muscularised vessels in rat lung and (B) wall thickness of larger, fully muscularised pulmonary arterioles. For (A), statistical significance was assessed by comparing the percentage of fully muscularised vessels between groups. For MCT treated animals, comparison of the effect of MM07 and saline was determined by Student's two-tailed *t*-test, *P≤0.05. Data are expressed as mean±sem.

Figure 7: MM07 activated endothelial nitric oxide synthase and AMP-activated protein kinase. (A) Stimulation of human PAECs with [Pyr^{1}]apelin-13 or MM07 increased the level of phosphorylated eNOS measured by chemiluminescence (n=11 each). (B) Stimulation of human PAECs with [Pyr^{1}]apelin-13 or MM07 increased the level of phosphorylated AMPKa measured by chemiluminescence (n=11 each). RLU, relative light units. *P≤0.05, as determined by repeated measures ANOVA with Dunnett's post-test. (C), Stimulation of human PAECs with [Pyr^{1}]apelin-13 or MM07 increased the level of mRNA of eNOS, as determined by one-way ANOVA with Tukey's post-test. Data are expressed as mean±sem.

Figure 8: MM07 promoted proliferation of pulmonary arterial endothelial cells. (A) Representative two-channel overlay photomicrographs of cells treated with PBS (baseline), rhVEGF (as a positive control), [Pyr^{1}]apelin-13 or MM07, showing EdU

negative cell nuclei in blue and EdU positive nuclei in cyan. Scale bar = 200μm. (B) Stimulation of human PAECs with rhVEGF, [Pyr^{1}]apelin-13 or MM07 increased the proportion EdU positive cells (n=6 each). *P≤0.05, as determined by a repeated measures ANOVA. Data are expressed as mean±sem.

Figure 9: Rescue of apoptosis of human pulmonary arterial endothelial cells induced by TNFα/CHX (n=8 independent experiments using cells from three donors). TNFα/CHX significantly induced apoptosis relative to the EBM-2 2%FBS serum and growth factor starved control ($^{\#}p<0.05$). rhVEGF pre-treatment for 18 hours significantly attenuated this apoptotic induction as did MM07. *P≤0.05, as determined by a repeated measures ANOVA. Data are expressed as mean±sem.

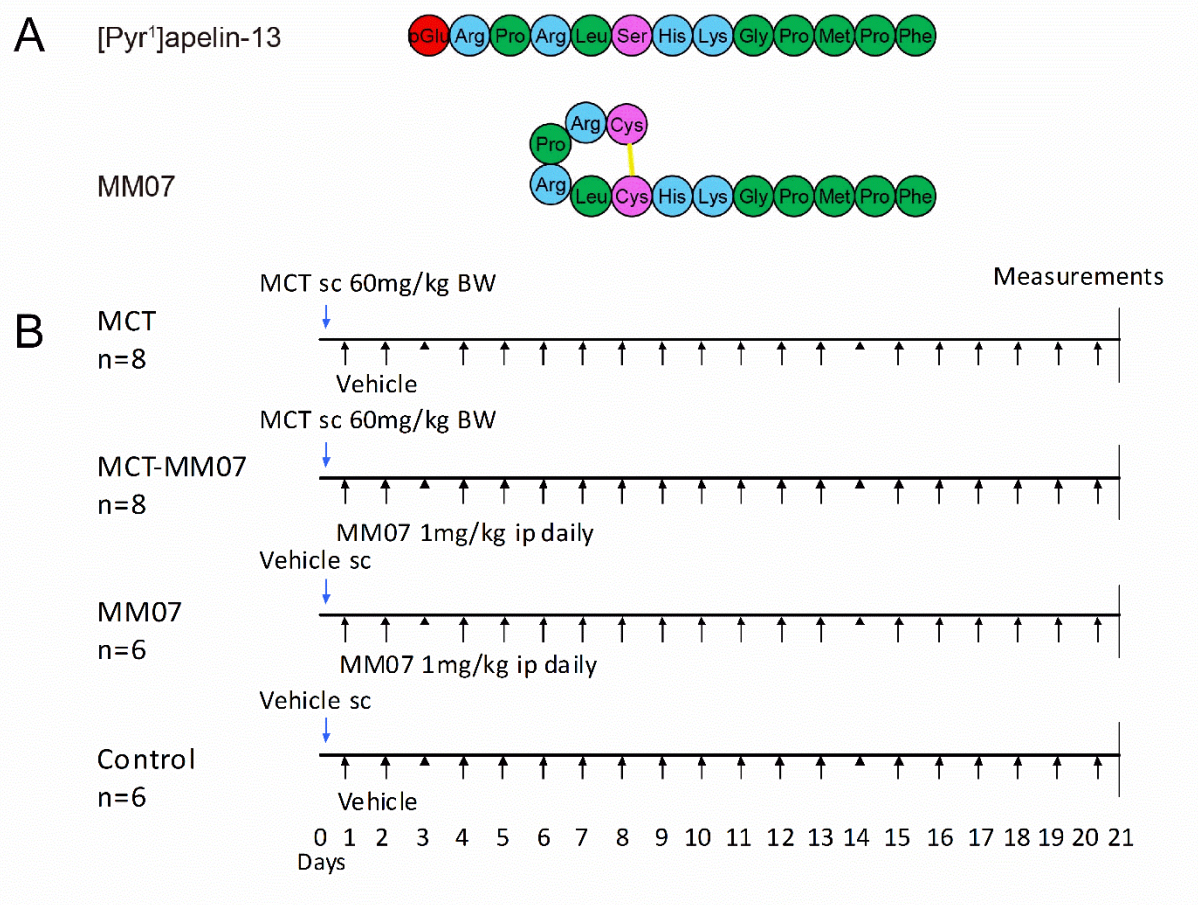
A
[Pyr1]apelin-13
pGlu Arg Pro Arg Leu Ser His Lys Gly Pro Met Pro Phe
MM07
Arg Cys Pro Arg Leu Cys His Lys Gly Pro Met Pro Phe
B
MCT sc 60mg/kg BW
Measurements
MCT
n=8
Vehicle
MCT sc 60mg/kg BW
MCT-MM07
n=8
MM07 1mg/kg ip daily
Vehicle sc
MM07
n=6
MM07 1mg/kg ip daily
Vehicle sc
Control
n=6
Vehicle
0 1 2 3 4 5 6 7 8 9 10 11 12 13 14 15 16 17 18 19 20 21
Days

Figure 1

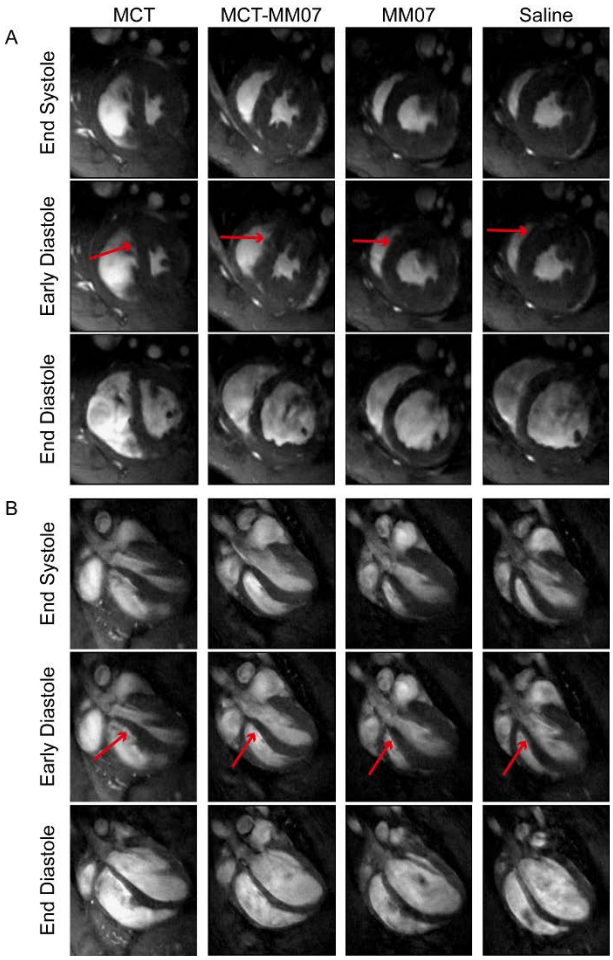
MCT
MCT-MM07
MM07
Saline
A
End Systole
Early Diastole
End Diastole
B
End Systole
Early Diastole
End Diastole

Figure 2

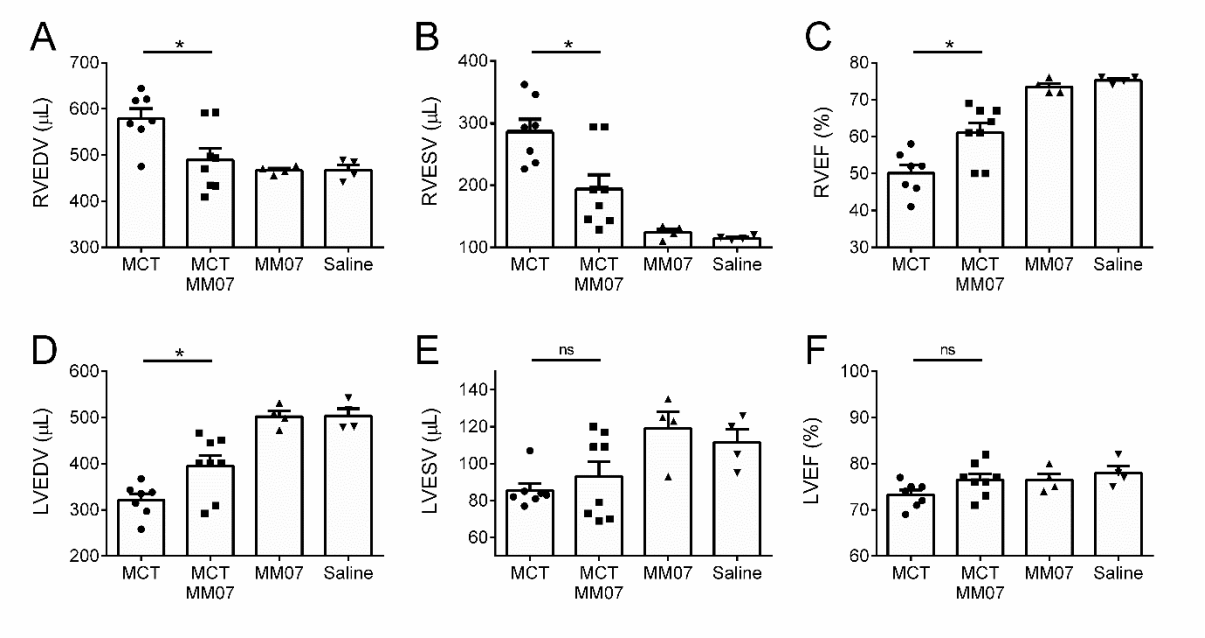
A
RVEDV (µL)
700
600
500
400
300
*
MCT
MCT MM07
MM07
Saline
B
RVESV (µL)
400
300
200
100
*
MCT
MCT MM07
MM07
Saline
C
RVEF (%)
80
70
60
50
40
30
*
MCT
MCT MM07
MM07
Saline
D
LVEDV (µL)
600
500
400
300
200
*
MCT
MCT MM07
MM07
Saline
E
LVESV (µL)
140
120
100
80
60
ns
MCT
MCT MM07
MM07
Saline
F
LVEF (%)
100
90
80
70
60
ns
MCT
MCT MM07
MM07
Saline

Figure 3

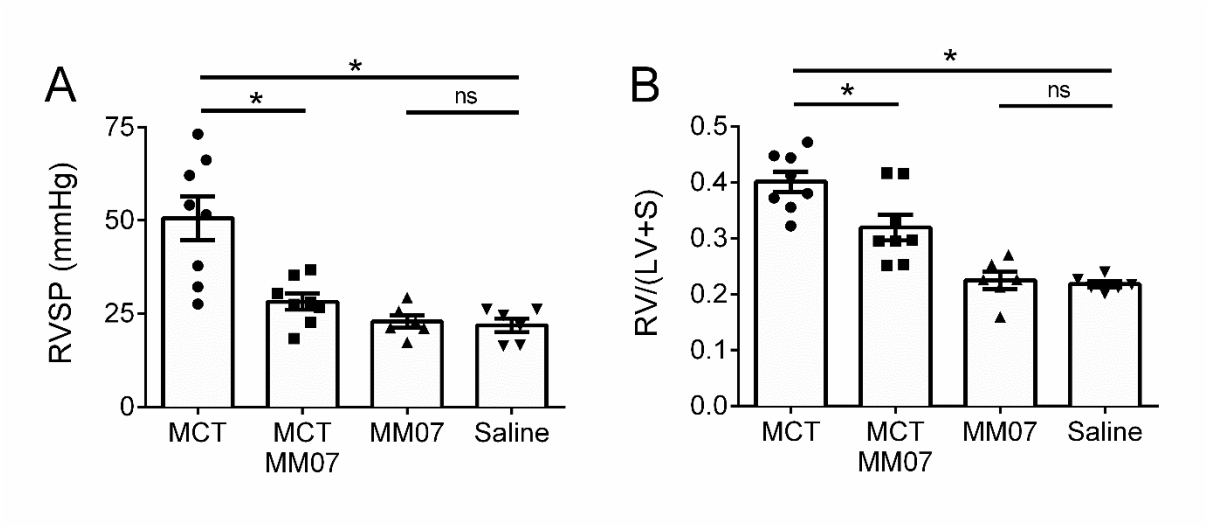
A
*
*
ns
RVSP (mmHg)
75
50
25
0
MCT
MCT MM07
MM07
Saline
B
*
*
ns
RV/(LV+S)
0.5
0.4
0.3
0.2
0.1
0.0
MCT
MCT MM07
MM07
Saline

Figure 4

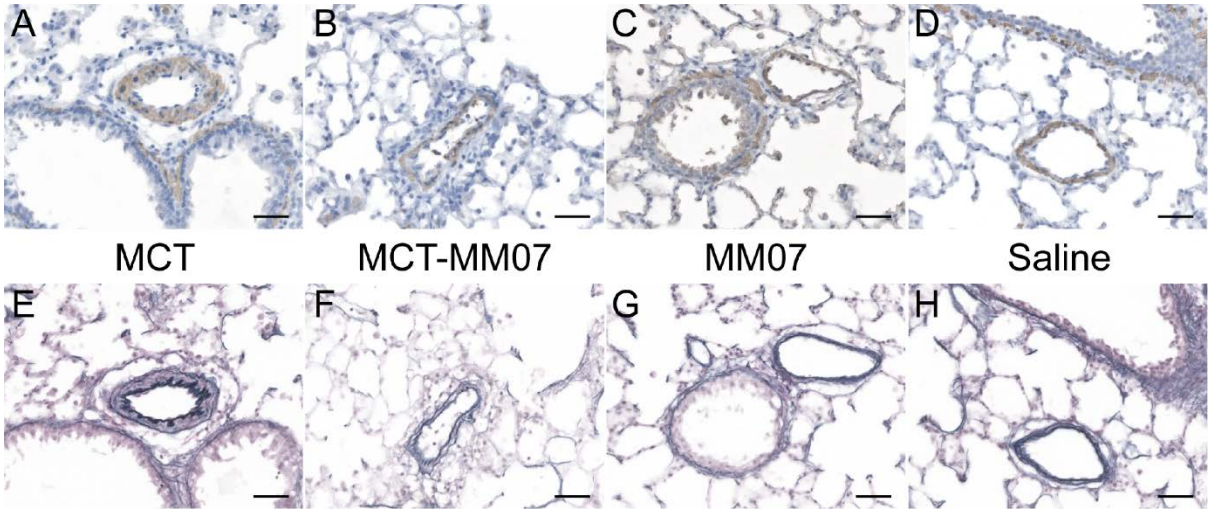

Figure 5

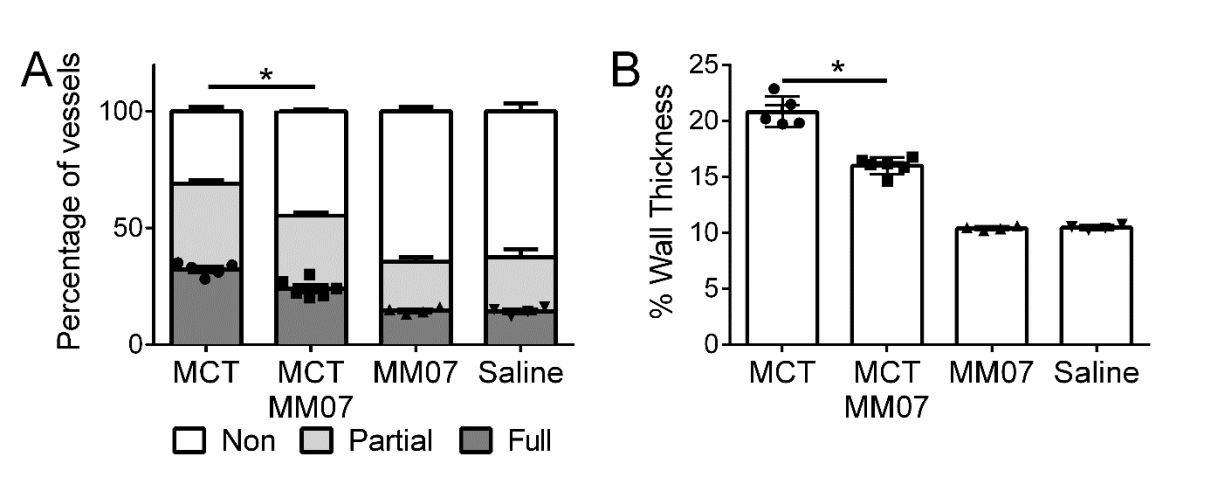
A
Percentage of vessels
100
50
0
*
MCT
MCT MM07
MM07
Saline
Non
Partial
Full
B
% Wall Thickness
25
20
15
10
5
0
*
MCT
MCT MM07
MM07
Saline

Figure 6

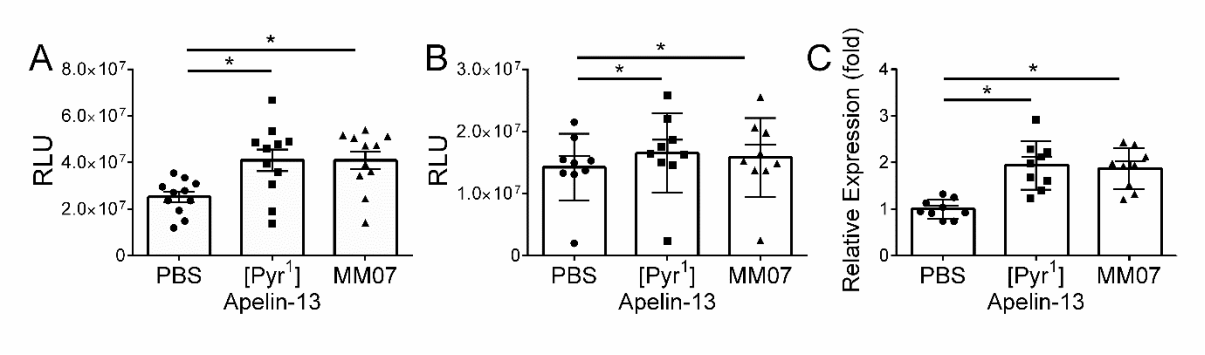
A
RLU
8.0×10^7
6.0×10^7
4.0×10^7
2.0×10^7
0
*
*
PBS
[Pyr^1]
MM07
Apelin-13
B
RLU
3.0×10^7
2.0×10^7
1.0×10^7
0
*
*
PBS
[Pyr^1]
MM07
Apelin-13
C
Relative Expression (fold)
4
3
2
1
0
*
*
PBS
[Pyr^1]
MM07
Apelin-13

Figure 7

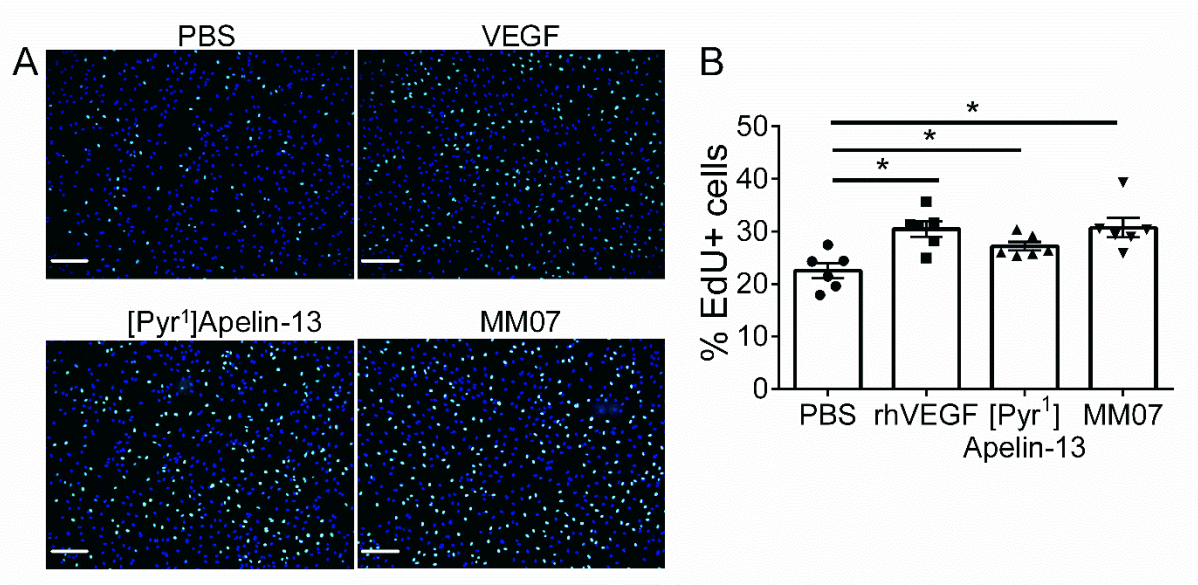
A
PBS
VEGF
[Pyr1]Apelin-13
MM07
B
% EdU+ cells
50
40
30
20
10
0
*
*
*
PBS
rhVEGF
[Pyr1] Apelin-13
MM07

Figure 8

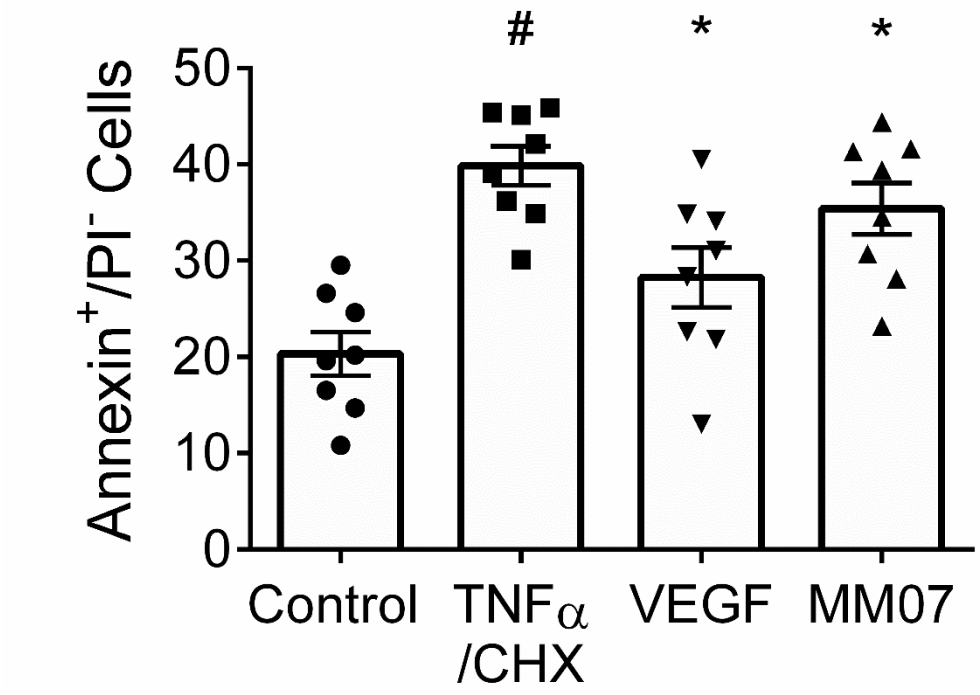

Figure 9